## MICONAZOLE NITRATE TABLETS

### 6.2.1 Preformulation studies

### Screening studies

The characterization of drugs and polymers were carried out using DSC and FT-IR. DSC thermogram and FT-IR spectra of pure MN is again mentioned in screening studies to avoid inconvenience and for easy comparison.

**a. Differential Scanning Calorimetry (DSC):** DSC studies were carried out for miconazole nitrate (MN) and its combination with polymers in 1:1 ratio and the thermograms obtained are presented in Figures 45 and 46. From the thermograms it was evident that decomposition temperature of miconazole nitrate (182 °C) was not changed when a mixed with excipients (182.18 °C). Hence, it may be inferred that there is no interaction between miconazole nitrate and polymers used in the preparation of tablets.

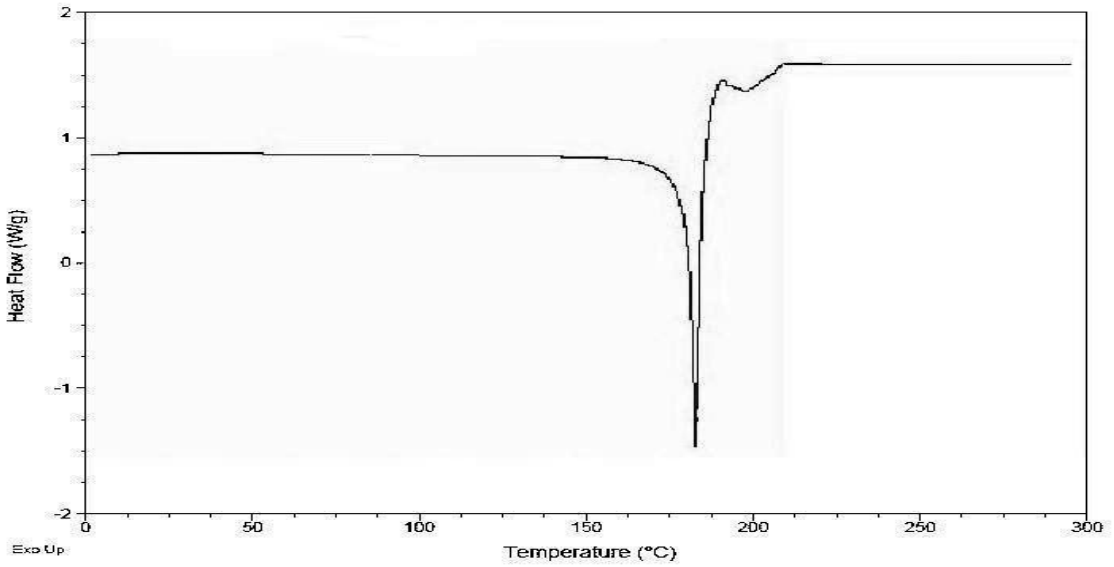


**Figure 45: DSC thermogram of miconazole nitrate (MN)**

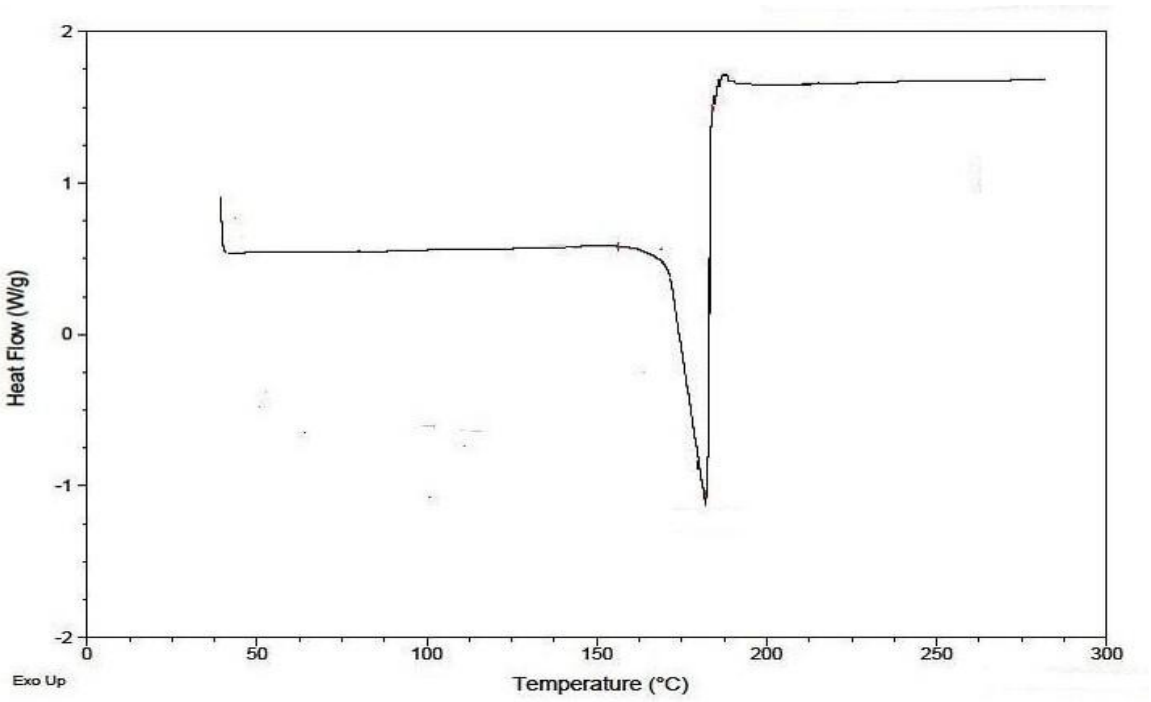


**Figure 46: DSC thermogram of miconazole nitrate (MN) with excipients**

**b. Fourier transform infrared spectroscopy:** The compatibility between the drug and polymer was compared by FT-IR spectra. The position of peak in FT-IR spectra of pure Miconazole nitrate was compared with those in FT-IR spectra of Miconazole nitrate with excipients. It was observed that, there was no disappearance or shift in peak position of Miconazole nitrate in any spectra of drug and excipients, which proved that drug and excipients were compatible. Hence, it can be concluded that drug can be used with polymer selected without causing instability in the formulation. The data obtained is shown in Table 20. The spectra are reported in Figures 47 and 48.

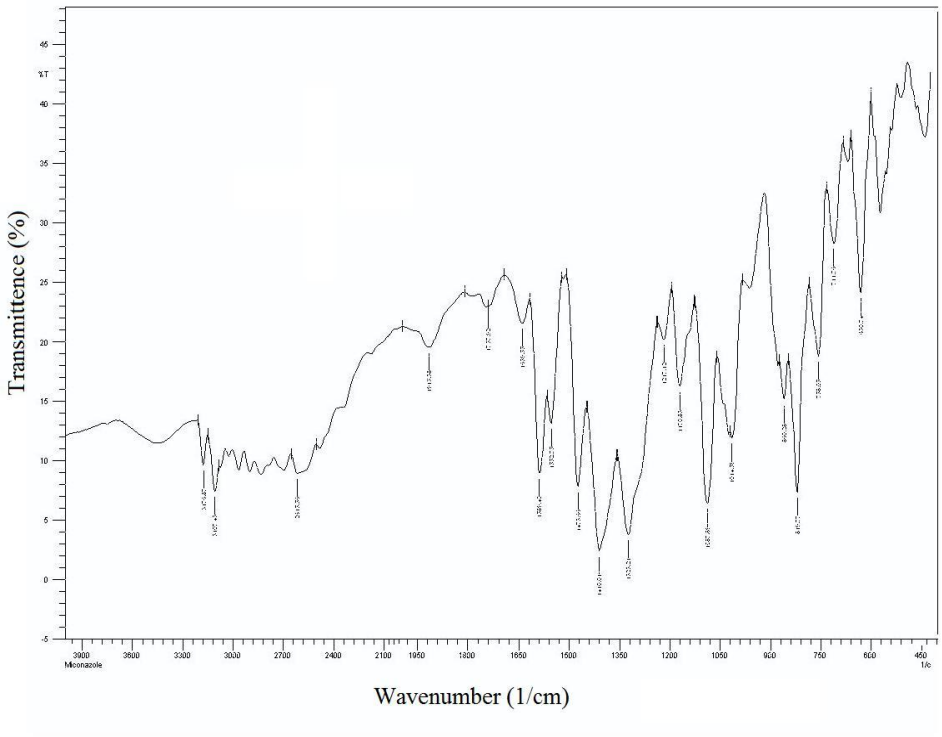


**Figure 47: FT-IR Spectra of pure Miconazole nitrate (MN)**

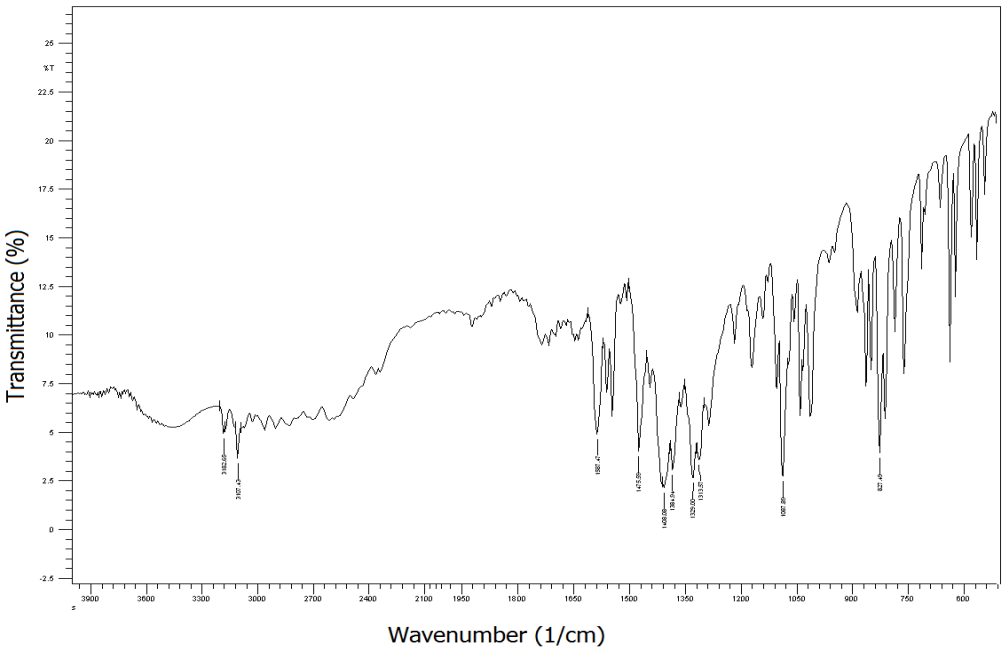


**Figure 48: FT- IR Spectra of miconazole nitrate (MN) with excipients**

**Table 20: FT-IR spectra data of Miconazole nitrate (MN) and the formulation.**

| Group | Frequency (in $cm^{-1}$) | |
|---|---|---|
| | **Drug** | **Formulation** |
| Aromatic | | |
| C-H stretching | 3181.1 | 3182.8 |
| C-C stretching | 1588.0 | 1587.4 |
| Combination | 1921.1 | 1920.5 |
| Aliphatic | | |
| C-H stretching | 2826.2 | 2824.3 |
| C-H bending | 1474.8 | 1475.59 |
| N-H stretching | 3440.13 | 3443.15 |
| Ether C-O-C stretching | 1088.1 | 1086.6 |
| $NO_2$ bending | 1313.21 | 1313.57 |
| C-Cl stretching | 713.6 | 712.9 |

### 6.2.2 Viscosity study of chitosan-carboxymethyltamarind (CMT) IPEC ratios

The viscosity of the supernatants obtained after mixing solution of chitosan with CMT solution in different ratios. CMT bears a negative charge owing to the presence of -COO− group introduced in CMT by carboxymethylation. Chitosan bears a net positive charge due to presence of $–NH_3^+$ groups. As a result, both polymers undergo spontaneous reaction when mixed together, resulting in formation of a solid mass. It was observed that the viscosity of the supernatant obtained after mixing aqueous solutions of chitosan and CMT decreased as the proportion of chitosan in chitosan-CMT mixtures decreased [190]. The minimum viscosity of the supernatant obtained by reacting chitosan and CMT in the ratio of 2:2 indicated maximum interaction.

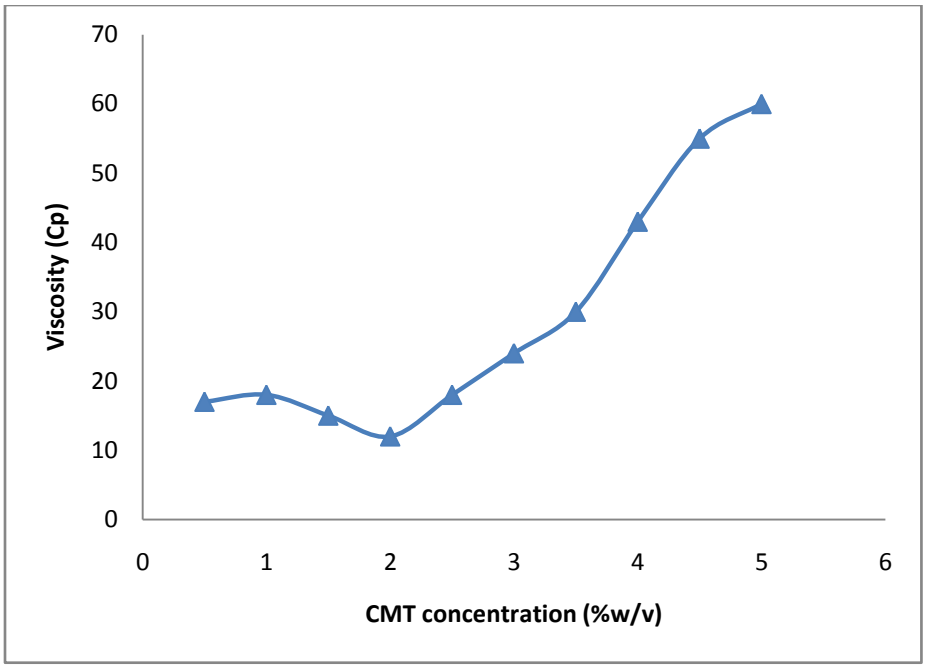


**Figure 49: Viscosity of the supernatant solutions of different ratios of chitosan and CMT**

### 6.2.3 Characterization of the chitosan-CMT IPEC

#### 6.2.3.1 Fourier transform infrared spectroscopy (FT-IR)

FT-IR study indicated that interpolymer complex could be formed by the electrostatic interaction between the $COO^-$ group of CMT and $NH_3^+$group of chitosan. The protonation of chitosan and dissociation of CMT solution was successfully accomplished by dissolving solution of chitosan and CMT acetic acid solution and water, respectively. Subsequently, the chitosan and CMT interpolyelectrolyte complex was prepared with those solutions.

The degree of deacetylation of chitosan is 85 %, the amine group of the 2-aminoglucose unit and the carbonyl group of the 2- acetaminoglucose unit of chitosan showed absorption bands at 1575 and 1656 $cm^{-1}$, respectively and the band at 1380 $cm^{-1}$

represents –CH2 bending. The absorption bands at 1160 $cm^{-1}$ (anti-symmetric stretching of the C–O–C bridge), 1075 and 1040 $cm^{-1}$ (skeletal vibrations involving the C–O stretching) are characteristics of its saccharide structure. The FT-IR spectra of chitosan in 2000-1000 $cm^{-1}$ and 1800-1400 $cm^{-1}$ are given in figure 27 and 28 respectively.

The spectrum of CMT showed the characteristic absorption band at 1743 $cm^{-1}$ corresponds to ester carbonyl group are attributed to its saccharide structure [191]. FTIR spectra of CMT in 2000-1000 $cm^{-1}$ and 1800-1400 $cm^{-1}$ are given in figure 50 and 51 respectively.

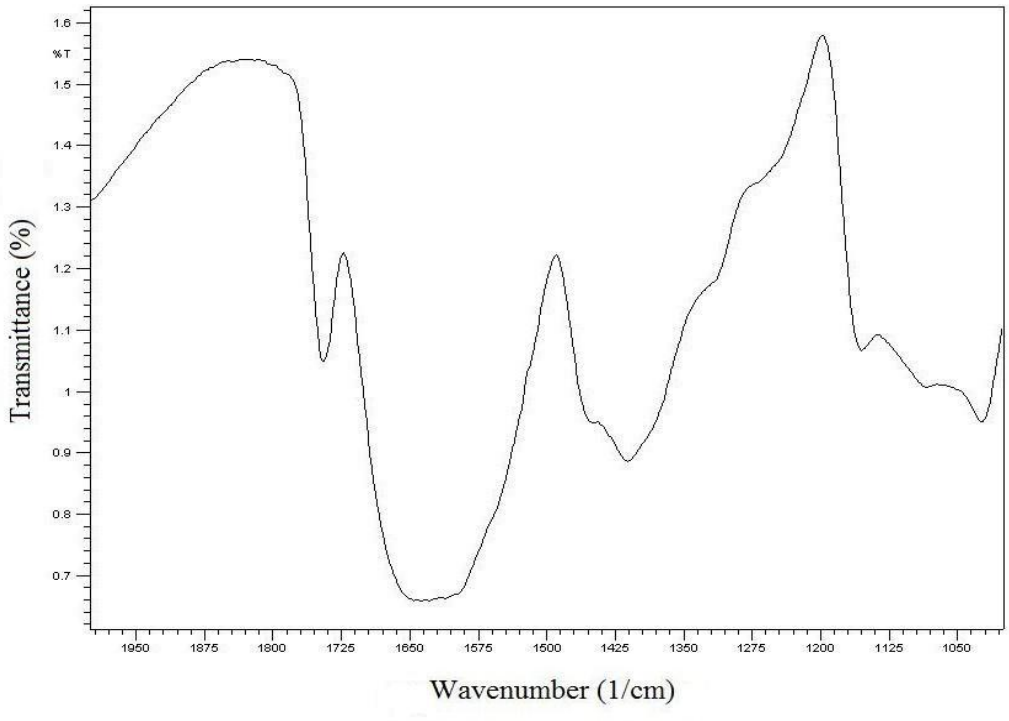


**Figure 50: FT-IR spectra of CMT in 2000-1000 $cm^{-1}$**

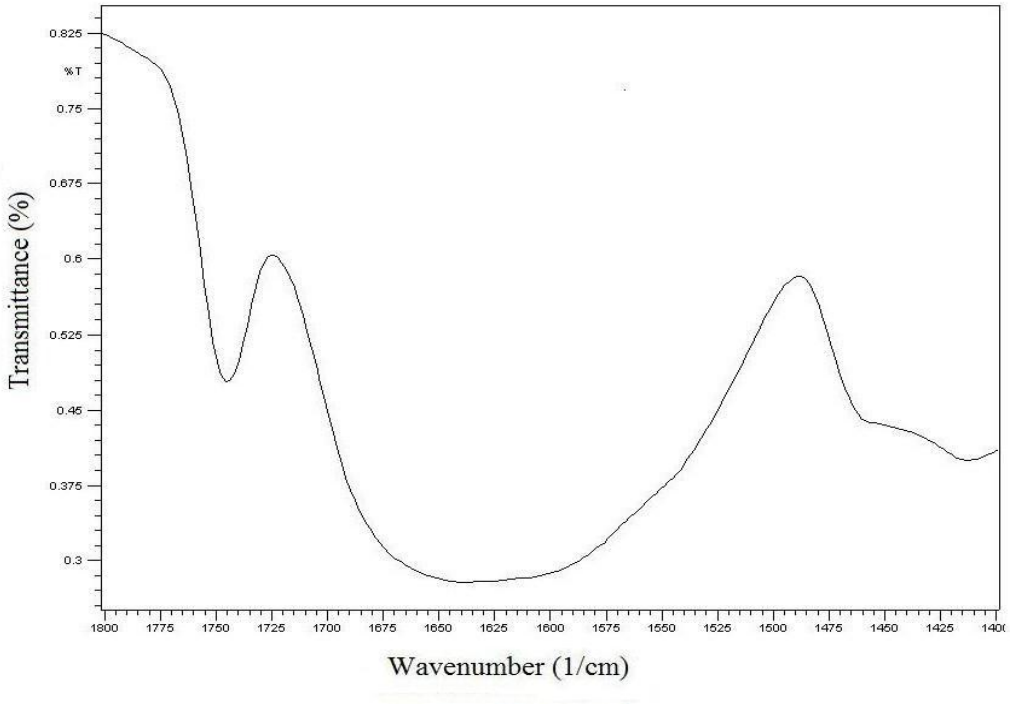


**Figure 51: FT-IR spectra of CMT in 1800-1400 $cm^{-1}$**

The FT-IR spectra of IPEC in 2000-1000 $cm^{-1}$ and 1800-1400 $cm^{-1}$ are given in figure 52 and 53 respectively. FT-IR spectrum of chitosan employed in this study showed doublet peaks of amide bond at 1656 and 1575 $cm^{-1}$ as it was obtained from partial N-deacetylation of chitin. However, these doublet peaks changed into nearly singlet band at 1651 $cm^{-1}$ in IPEC with an increase in sharpness of band. The peak of methyl carbonyl groups at 1743 $cm^{-1}$ also diminished as compared to the CMT [192]. This difference in IR spectrum of complex may be attributed to the possibility of association between CMT and chitosan due to electrostatic interaction.

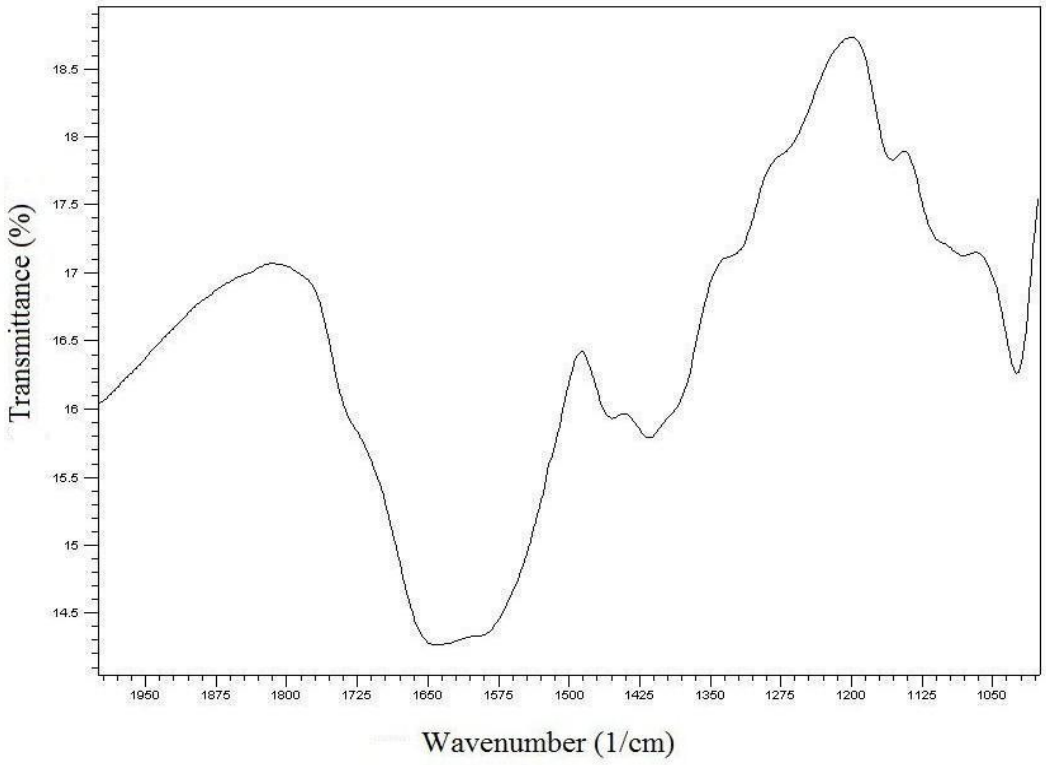


**Figure 52: FT-IR spectra of chitosan-CMT IPEC in 2000-1000 cm$^{-1}$**

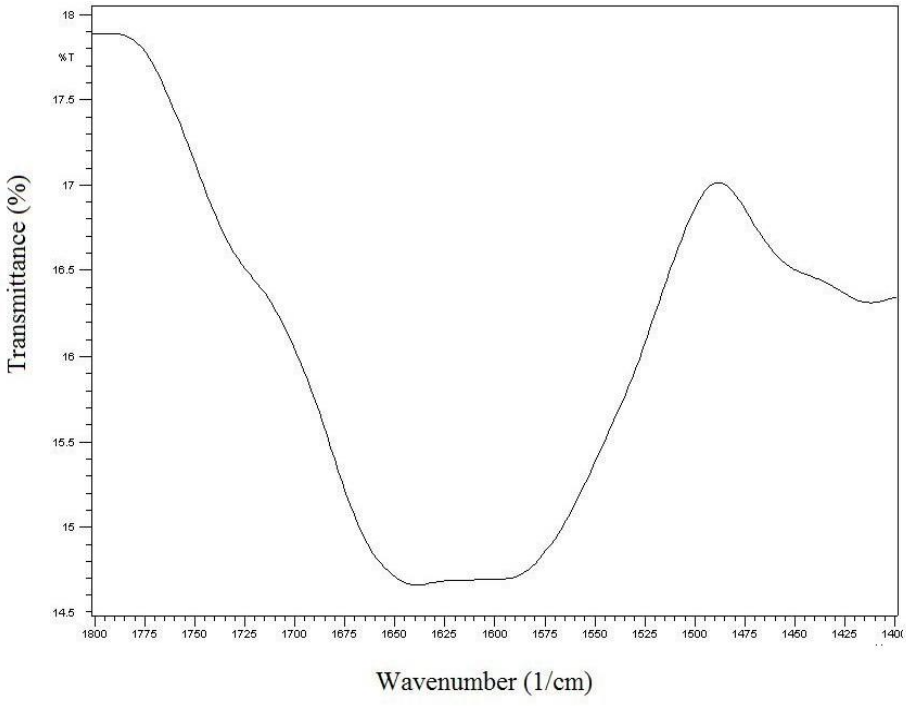


**Figure 53: FT-IR spectra of chitosan-CMT IPEC in 1800-1400 cm$^{-1}$**

### 6.2.3.2 Differential scanning calorimetry (DSC)

Chitosan exhibits an endothermic peak around 100 °C and exothermic peak at 320 °C. The peak at 100 °C was attributed to the evaporation of absorbed water, and the peak around 320 °C was probably due to the first step of chitosan degradation. The peak at 320 °C is the characteristic peak of chitosan. Chitosan pyrolysis starts by a random split of the glycosidic bonds, followed by further decomposition to acetic, butyric and lower fatty acids. The DSC thermogram of chitosan was shown in figure 33.

The DSC thermogram of CMT exhibit endothermic peak at 120 °C and an exothermic peak near 300 °C. The endothermic peak is due to the bound water and the polymer start to degrade after 300 °C. The CMT thermogram is shown in figure 54.

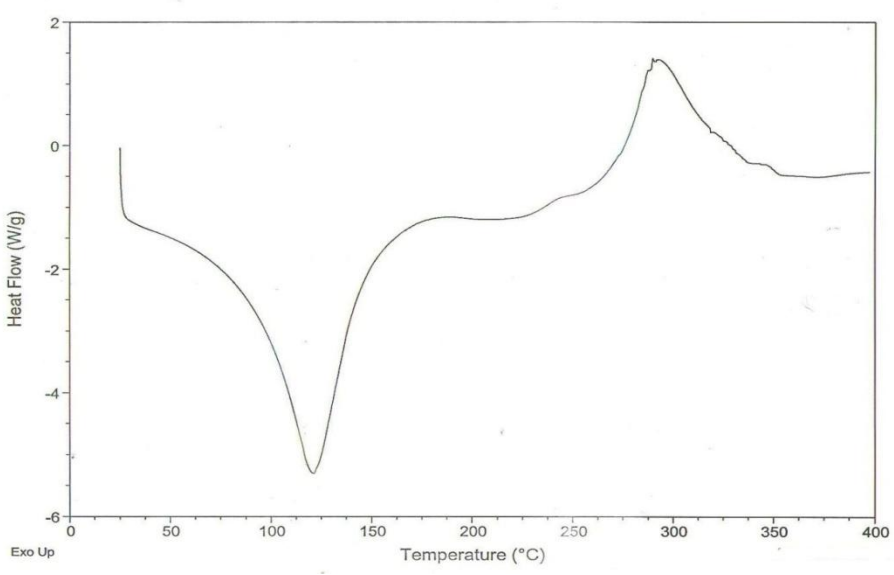


**Figure 54: DSC thermogram of CMT**

DSC thermogram of IPEC is given in figure 55. Although the IPEC thermogram showed endothermic peak at 100 °C and exothermic peak at 230 °C. DSC study of chitosan, CMT and IPEC showed distant change in position of exothermic peak. The significant changes in the position of peaks in thermogram of polymers imply that the formed product is

complex (different product) and just not the mixture of chitosan and CMT.

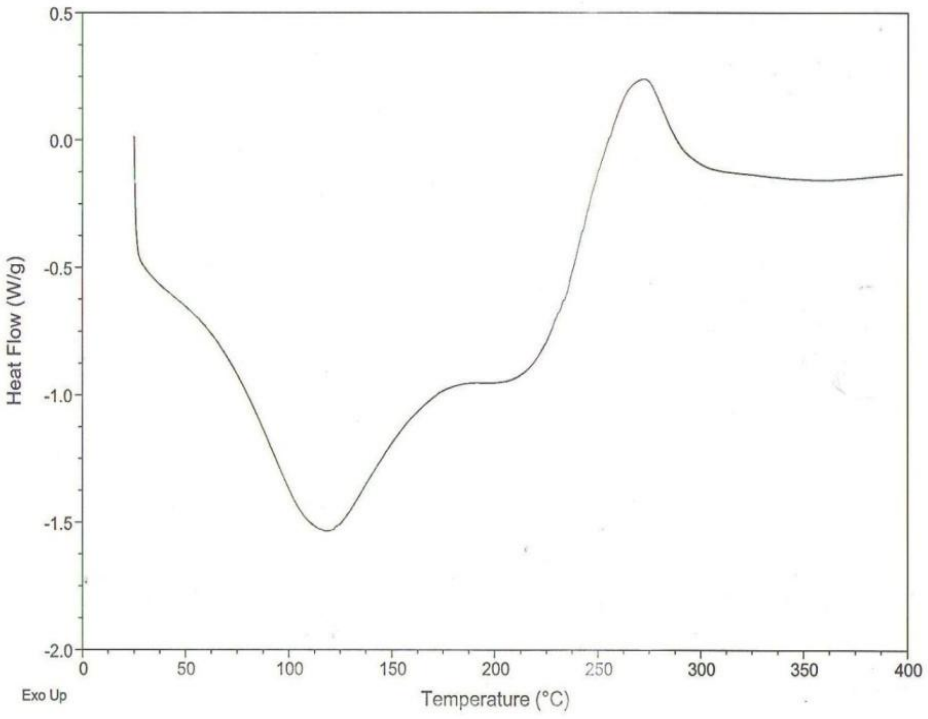


**Figure 55: DSC thermogram of chitosan-CMT IPEC**

### 6.3.2.3 X-ray diffraction (XRD)

The X-ray diffraction pattern of chitosan is presented in figure 36. The X-ray diffraction pattern of chitosan powder showed two prominent diffraction peaks at 11° (2θ) and 20° (2θ). A shoulder peak appears at 22° and also a minor peak appears at 27°. The two prominent crystalline peaks at 11° and 20° are typical fingerprints of chitosan which are related to the hydrated and anhydrous crystals respectively.

The x-ray diffraction pattern of CMT is shown in figure 56. The X-ray diffraction pattern of CMT powder showed prominent diffraction peak at 20° (2θ) and minor peak appeared at 29° (2θ).

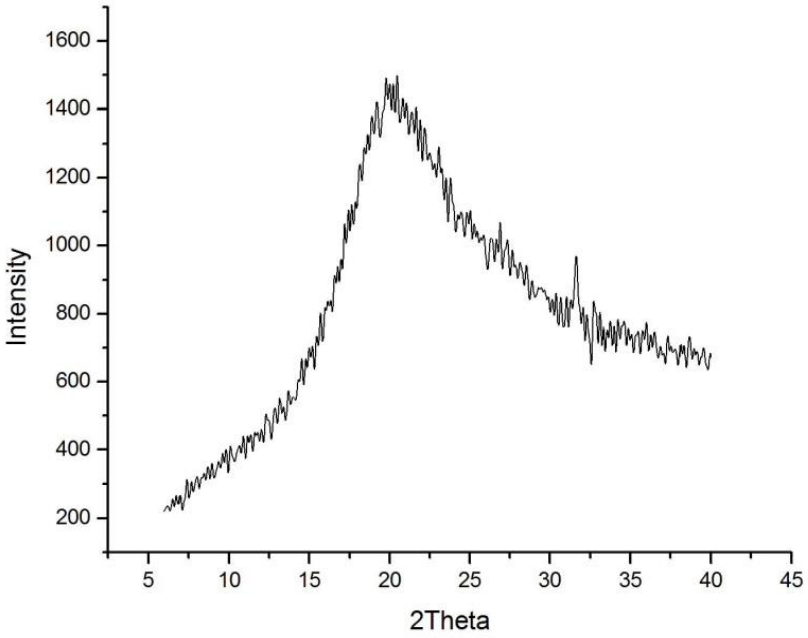


**Figure 56: X-ray diffraction spectra of CMT**

IPEC X-ray diffraction pattern is given in figure 57. The X-ray diffraction pattern of IPEC powder shows prominent diffraction peak at 21°. After complexing, the typical peaks of chitosan disappeared and this suggested that the introduction of CMT into chitosan disrupted the crystalline structure of chitosan, hindering the formation of hydrogen bonding between amino groups and hydroxyl groups. The broad amorphous pattern of the IPEC indicates a good compatibility and strong interaction between CMT and chitosan with a complete dispersion of chitosan chains. These intermolecular interactions could prevent macromolecules to crystallize individually as reported for some interpolymer complexes [193-196].

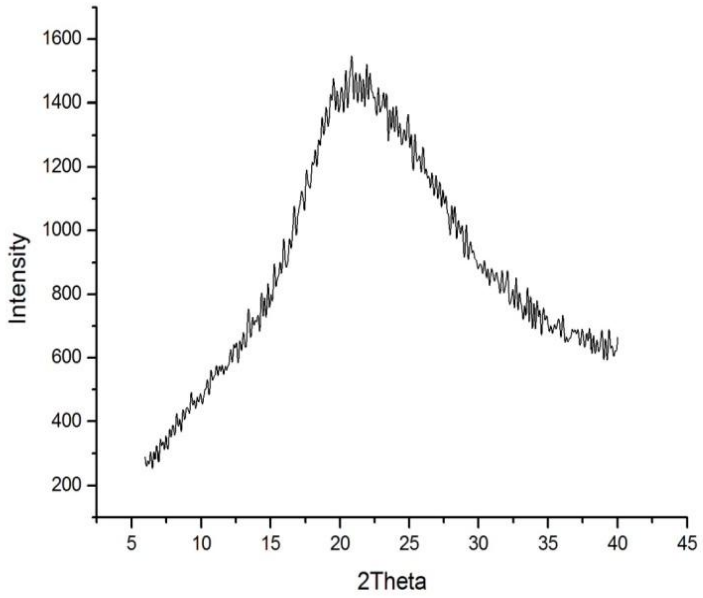


**Figure 57: X-ray diffraction spectra of chitosan-CMT IPEC**

### 6.2.4 Evaluation of matrix tablets containing miconazole nitrate (MN)

**Tablet properties**

The experimental results of tablet evaluation parameters are summarized in table 21. The weights of the prepared tablets were in the range of 149.3-150.3 mg. Tablets of all the batches complied with the weight variation requirement of Indian pharmacopeia and no batch varied more than 10% of the average weight indicating consistency in the preparation of tablet with minimal variation from batch to batch [182]. Thickness of all the tablet formulations ranged from 2 to 2.03 mm. Hardness of the tablets ranged between 61-75 N. All the tablet formulations exhibited friability less than 1%, indicating compliance with the requirement of USP 29 [183].

**Table 21: Evaluation data of MN matrix tablets**

| Formulation code | Weight (mg)* (n=20) | Thickness (mm)* (n=20) | Hardness (N)* (n=10) | Friability (%) (n=20) | %Drug content* (n=3) |
|---|---|---|---|---|---|
| MF1 | 150.3±0.51 | 2.0±0.02 | 63±3 | 0.18 | 99.93±0.02 |
| MF2 | 149.3±0.45 | 2.01±0.02 | 61±2 | 0.19 | 99.90±0.05 |
| MG1 | 149.5±0.37 | 2.02±0.01 | 71±4 | 0.09 | 99.91±0.02 |
| MG2 | 149.2±0.63 | 2.01±0.01 | 74±5 | 0.02 | 99.92±0.01 |
| MH1 | 150.2±0.24 | 2.01±0.02 | 68±2 | 0.07 | 99.93±0.05 |
| MH2 | 149.8±0.32 | 2.02±0.01 | 70±3 | 0.05 | 99.91±0.04 |
| MH3 | 149.3±0.88 | 2.02±0.01 | 74±2 | 0.09 | 99.89±0.15 |
| MH4 | 150.3±0.34 | 2.03±0.02 | 75±4 | 0.07 | 99.90±0.11 |
| MI1 | 150.0±0.94 | 2.02±0.02 | 70±2 | 0.07 | 99.92±0.12 |
| MI2 | 149.3±0.42 | 2.01±0.01 | 72±4 | 0.09 | 99.93±0.01 |
| MI3 | 150.5±0.53 | 2.02±0.02 | 71±3 | 0.02 | 99.95±0.05 |
| MI4 | 150.0±0.44 | 2.02±0.01 | 70±3 | 0.02 | 99.94±0.02 |

*mean± Standard Deviation

### 6.2.5 Swelling studies

The swelling studies were carried out in phosphate buffer pH 6.8 and simulated vaginal fluid pH 4.2. Chitosan polymer behavior in phosphate buffer pH 6.8 and simulated vaginal pH 4.2 is as discussed under first part of the work and the chitosan fails to attain the desired swelling and *in vitro* drug release studies. Hence the chitosan polymer alone is not included in this study.

The influence of pH value of the buffer solution on the swelling behavior of formulations at 37±0.5 °C in phosphate buffer pH 6.8 and simulated vaginal fluid pH 4.2 are given in table 22, 23 and graphically represented in Figure 58A, 58B and 59A, 59B respectively. The swelling ratios of tablet formulations at various pH environments depend upon the available free volume of the expanded polymer matrix, polymer chain relaxation, and availability of ionizable functional groups such as –COOH able to form hydrogen bonds with dissolution medium.

Formulations MF1 and MF2 containing carboxymethyl tamarind exhibit less swelling in simulated vaginal fluid pH 4.2 than in phosphate buffer pH 6.8. There is a gradual increase in swelling in vaginal pH 4.2, because the pKa of any polymer containing carboxylic acid is about 4.5, and carboxyl groups of CMT tends to dissociate at a pH > 4.5 and the osmotic pressure inside the hydrogels increases. Therefore, gradual rise in swelling occurred in the vaginal pH. However increased for more dissociation of carboxylic acid was observed in phosphate buffer pH 6.8 as compared to SVF pH 4.2, which led to higher swelling. Higher concentration of CMT leads to a slight swelling index in phosphate buffer pH 6.8. The swelling study results of carboxyl containing polymers in acidic to neutral pH exhibit gradual swelling were in agreement with the

reported studies [197]. The physical mixture of chitosan and CMT polymer formulations exhibit relatively varied swelling index in vaginal pH 4.2 and phosphate buffer pH 6.8. In physical mixture free functional group were available to the dissolution medium which resulted in varied swelling index. In phosphate buffer pH 6.8, dissociation of carboxymethyl group of CMT and deprotonation of amine group of chitosan occurs. This may lead to weaker electrostatic interaction and lesser attraction of polymer chains leading more opened structure resulting in higher swelling index. In simulated vaginal pH 4.2, the amine group of chitosan is less protonated to $-NH_3^+$ group because chitosan protonation increase will be more in acidic pH. As pH increases or to neutral pH, there is less protonation of amine group. There is electrostatic interaction of carboxyl group of CMT with protonated group of chitosan which caused a tightening of network resulting in less swelling [198]. IPEC containing tablet formulations exhibited almost similar swelling index in both phosphate buffer pH 6.8 and in simulated vaginal fluid pH 4.2. The similarity swelling profiles in both the buffer solutions may be attributed to the lack of availability of free functional group as in physical mixture of polymers or single polymers. MH1-MH4 formulations containing IPEC exhibited lesser swelling index than MG1 and MG2 formulations. The decreased swelling index of IPEC might be due to the intra molecular hydrogen bonding between the carboxymethyl groups of CMT and amine groups of chitosan or hydroxyl group or carboxymethyl groups may occur elsewhere in the network as suggested earlier [199]. This hydrogen bonding may also result in tightening of IPEC network leading to a reduced swelling capacity.

The addition of polymers to IPEC alters the swelling index in both phosphate buffer pH 6.8 and simulated vaginal fluid pH 4.2. The availability of free functional groups

produces either strong or weak electrostatic interaction leading to change in swelling index. MI1 formulation containing CMT along with IPEC exhibited a little higher swelling index initially as explained earlier. Whereas in case of MI2 formulation, the presence of chitosan and CMT doesn't alter swelling index much, due to the opposing action and a higher concentration of IPEC. Last two formulations also exhibited varied swelling capacity but the strong polymeric network of IPEC doesn't have much impact.

**Table 22: Swelling index data of MN formulations MF1-MI4 in phosphate buffer pH 6.8**

| Formulation Code | Swelling index Mean ± S.D* | | | | | | | |
|---|---|---|---|---|---|---|---|---|
| | Time in Hours | | | | | | | |
| | 1 hour | 2 hour | 3 hour | 4 hour | 5 hour | 6 hour | 7 hour | 8 hour |
| MF1 | 40 ±0.65 | 89 ±0.14 | 145 ±0.56 | 178 ±0.37 | 296 ±0.42 | 352 ±0.15 | --- | --- |
| MF2 | 65 ±0.32 | 152 ±0.27 | 246 ±0.97 | 301 ±0.27 | 396 ±0.22 | 409 ±0.17 | --- | --- |
| MG1 | 83 ±0.53 | 176 ±0.27 | 251 ±0.18 | 326 ±0.71 | 411 ±0.83 | 432 ±0.29 | --- | --- |
| MG2 | 98 ±0.18 | 198 ±0.62 | 287 ±0.41 | 354 ±0.29 | 443 ±0.92 | 452 ±0.19 | --- | --- |
| MH1 | 91 ±0.57 | 106 ±0.29 | 123 ±0.38 | 189 ±0.46 | 219 ±0.11 | 265 ±0.15 | 283 ±0.25 | 327 ±0.36 |
| MH2 | 97 ±0.47 | 112 ±0.83 | 124 ±0.29 | 198 ±0.78 | 238 ±0.92 | 287 ±0.37 | 327 ±0.92 | 364 ±0.65 |
| MH3 | 102 ±0.52 | 126 ±0.73 | 175 ±0.38 | 244 ±0.61 | 301 ±0.38 | 377 ±0.53 | 401 ±0.29 | 451 ±0.82 |
| MH4 | 105 ±0.75 | 154 ±0.38 | 207 ±0.72 | 272 ±0.88 | 322 ±0.28 | 402 ±0.17 | 426 ±0.82 | 472 ±0.17 |
| MI1 | 130 ±0.13 | 225 ±0.51 | 261 ±0.17 | 301 ±0.82 | 365 ±0.93 | 421 ±0.45 | 440 ±0.37 | 451 ±0.83 |
| MI2 | 115 ±0.47 | 132 ±0.83 | 158 ±0.95 | 224 ±0.26 | 276 ±0.63 | 302 ±0.27 | 319 ±0.72 | 343 ±0.53 |
| MI3 | 105 ±0.15 | 126 ±0.35 | 185 ±0.73 | 245 ±0.61 | 297 ±0.36 | 339 ±0.11 | 392 ±0.25 | 423 ±0.71 |
| MI4 | 99 ±0.27 | 120 ±0.36 | 167 ±0.74 | 236 ±0.92 | 272 ±0.82 | 308 ±0.18 | 335 ±0.72 | 377 ±0.26 |

***Standard deviation, n = 3**

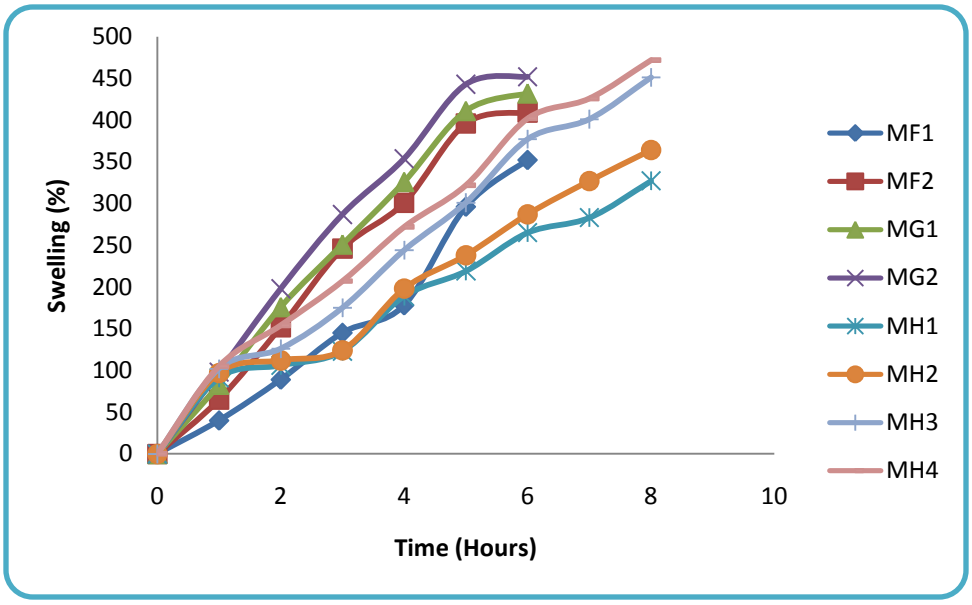


**Figure 58A: Swelling index profile for MN formulations MF1-MH4 in phosphate buffer pH 6.8**

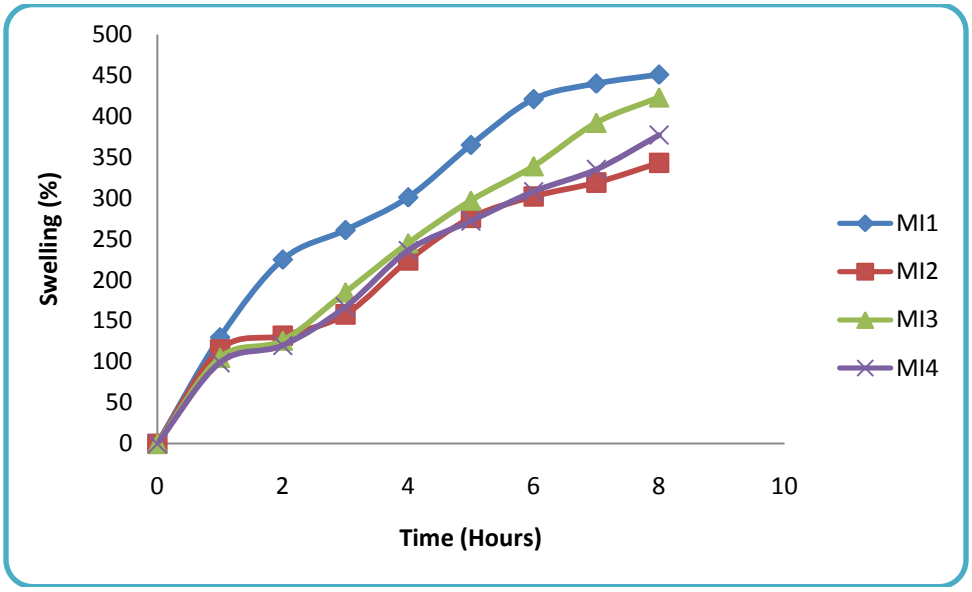


**Figure 58B: Swelling index profile for MN formulations MI1-MI4 in phosphate buffer pH 6.8**

**Table 23: Swelling index data of MN formulations MF1-MI4 in SVF pH 4.2**

| Formulation Code | Swelling index Mean ±S.D* | | | | | | | |
|---|---|---|---|---|---|---|---|---|
| | Time in Hours | | | | | | | |
| | 1 hour | 2 hour | 3 hour | 4 hour | 5 hour | 6 hour | 7 hour | 8 hour |
| MF1 | 25 ±0.71 | 56 ±0.14 | 102 ±0.48 | 168 ±0.92 | 201 ±0.27 | --- | ---- | ---- |
| MF2 | 40 ±0.19 | 97 ±0.76 | 154 ±0.17 | 208 ±0.95 | 276 ±0.81 | ---- | ---- | --- |
| MG1 | 55 ±0.83 | 135 ±0.45 | 197 ±0.27 | 255 ±0.33 | 303 ±0.38 | 357 ±0.51 | --- | --- |
| MG2 | 96 ±0.76 | 164 ±0.28 | 216 ±0.92 | 277 ±0.45 | 326 ±0.27 | 383 ±0.36 | --- | --- |
| MH1 | 88 ±0.34 | 102 ±0.73 | 125 ±0.17 | 185 ±0.29 | 222 ±0.72 | 259 ±0.36 | 293 ±0.46 | 317 ±0.27 |
| MH2 | 94 ±0.55 | 106 ±0.72 | 145 ±0.22 | 216 ±0.82 | 242 ±0.48 | 278 ±0.28 | 324 ±0.14 | 357 ±0.34 |
| MH3 | 101 ±0.48 | 130 ±0.73 | 167 ±0.46 | 236 ±0.21 | 272 ±0.17 | 318 ±0.73 | 365 ±0.28 | 397 ±0.71 |
| MH4 | 105 ±0.72 | 196 ±0.23 | 245 ±0.86 | 295 ±0.38 | 357 ±0.22 | 428 ±0.47 | 452 ±0.74 | 478 ±0.33 |
| MI1 | 125 ±0.47 | 223 ±0.34 | 252 ±0.42 | 298 ±0.62 | 354 ±0.48 | 416 ±0.37 | 443 ±0.28 | 445 ±0.92 |
| MI2 | 110 ±0.62 | 146 ±0.13 | 185 ±0.56 | 256 ±0.28 | 292 ±0.67 | 321 ±0.38 | 355 ±0.47 | 389 ±0.27 |
| MI3 | 115 ±0.47 | 176 ±0.38 | 235 ±0.68 | 275 ±0.59 | 337 ±0.72 | 389 ±0.26 | 412 ±0.11 | 428 ±0.23 |
| MI4 | 101 ±0.57 | 120 ±0.24 | 167 ±0.26 | 236 ±0.68 | 272 ±0.48 | 308 ±0.34 | 335 ±0.27 | 377 ±0.32 |

***Standard deviation, n = 3**

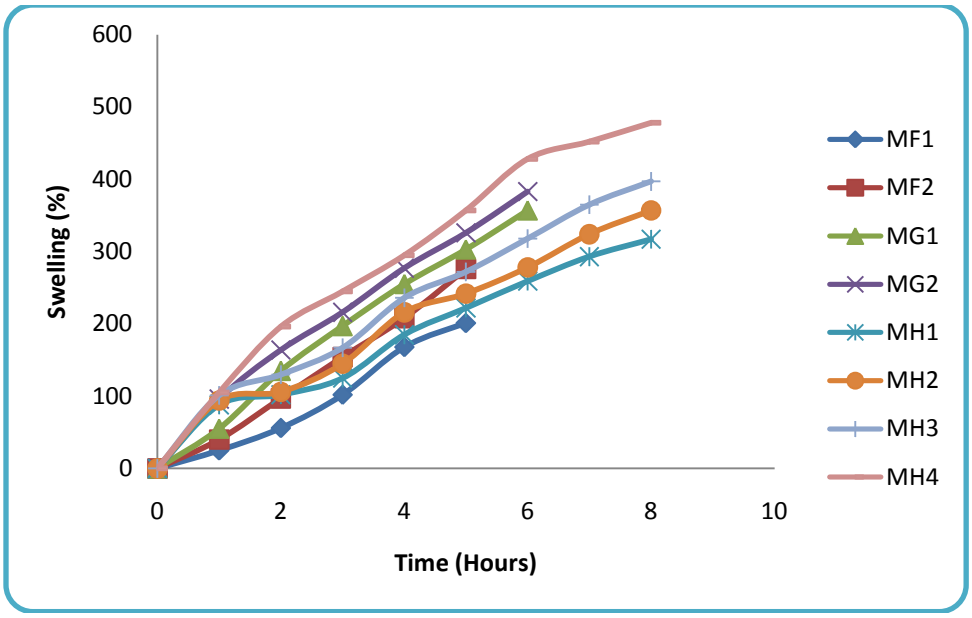


**Figure 59A: Swelling index profile for MN formulations MF1-MH4 in SVF pH 4.2**

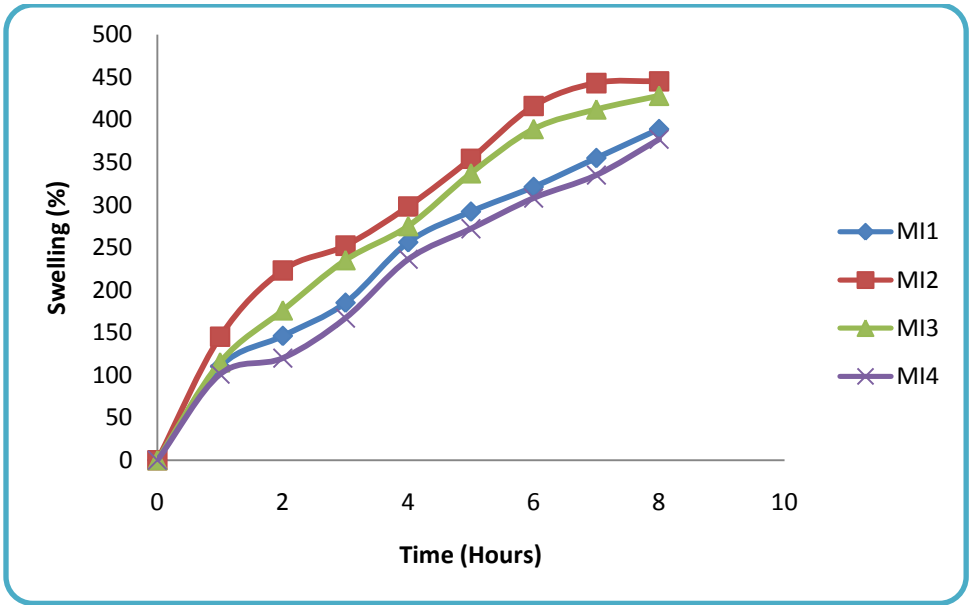


**Figure 59B: Swelling index profile for MN formulations MI1-MI4 in SVF pH 4.2**

### *6.2.6 In vitro* dissolution studies

In the previous chapter, chitosan alone does not seem suitable for desired drug release, because the transformation of the gel developed in acidic pH to a semi-solid form limited the drug release. The solid core of tablet was still compact in acidic pH and complete drug release was observed. On the other hand in buccal pH, the characteristic of chitosan is altered which may not be able to sustain the drug release profile.

The dissolution data of the individual formulations in phosphate buffer pH 6.8 and simulated vaginal fluid pH 4.2 are shown in the table 24 and 25 respectively and graphically represented in figures 60A, 60B and 61A, 61B respectively.

The release of miconazole from the MF1 formulation in simulated vaginal pH 4.2 is less than phosphate buffer pH 6.8. This may be due to the reason that CMT is ionized to a substantial level causing a tightening of polymeric network. This results in less swelling thus retarding drug release. Whereas in phosphate buffer pH 6.8, the rate of drug release is more due to suppressed ionization of CMT and also due to higher solubility of miconazole in phosphate buffer pH 6.8 than in simulated vaginal fluid pH 4.2 [200]. With increase in CMT concentration, the release of miconazole was enhanced, this may be due to the reason that CMT polymer promotes the entry of solution into the particles causing maximum swelling. This process increases the solubility of miconazole and thus accelerates its dissolution. The physical mixture of chitosan and CMT doesn't produce the desired drug release this may be due to faster disentanglement of the polymeric chains because polymers are not cross-linked with each other, relatively fast drug release. There is faster miconazole release from tablets based on chitosan-CMT powder mixture in phosphate buffer pH 6.8 than compared to that from those in simulated vaginal fluid pH

4.2. This indicates that CMT favors the tablet hydration and accelerates the diffusion of phosphate buffer pH 6.8 into the tablets. The dissolution results of chitosan-CMT powder mixture in SVF pH 4.2 represent the gradual drug release due to the ability of chitosan to form gel in acidic pH [201]. This indicates that although the tablets are based on dry blend of polymer powders, are not able to achieve the desired drug release. Inspite of miconazole being sparingly soluble in buffers the desired release rate from hydrophilic matrix was not achieved. Neither CMT nor chitosan, separately or in association, were able to control the release of miconazole in monolithic dosage form. The release rate of miconazole from IPEC matrix was lower than that from physical mixture or polymer alone; this is an interesting advantage for IPEC. IPEC containing formulation (MH1-MH4) upon contact with phosphate buffer pH 6.8 or simulated vaginal fluid undergo swelling-driven phase transition from a glassy state to rubbery state. Irrespective of buffer pH there is similar drug release profile from IPEC tablet formulation. This may be due to lack of availability of free functional groups in IPEC; hence the IPEC is not readily available for interaction with buffer pH like other polymers. The drug release rates are modulated by the rate of water transport and the thickness of the gel layer. Inspite of less swelling of IPEC than other individual polymers, the IPEC forms tight network thus able to release the miconazole slowly over a period of time. Increase in the concentration of IPEC in tablets further retard the drug release, a little due to the formation of still strong polymeric network. MI1 formulation containing CMT with IPEC exhibits the initial burst release of miconazole in phosphate buffer pH 6.8 due to suppressed ionization of CMT and further loosening the polymeric network. Therefore the rate of drug release from formulation is rapid. Whereas in vaginal pH 4.2, the CMT

further entangles with the polymeric network and there is slow pattern of drug release. Further addition of chitosan to IPEC along with CMT doesn't alter the release pattern, as both chitosan and CMT tend to diffuse from the IPEC along with the miconazole leading to interaction between amine group and carboxyl group in the polymeric network. The ready availability of functional group within the tight polymeric network of IPEC stop the passing of miconazole from formulations, thereby retarding the drug release pattern without any burst effect. Taken together, these results showed the advantage of IPEC for monolithic formulations. The IPEC excipients can bring about controlled release of miconazole in both buffer solutions. Presence of CMT in IPEC tablets has impact on drug release profile. However, addition of chitosan and CMT to IPEC matrix tablets doesn't alter the drug release profile.

To know the similarity of dissolution profiles of MI3 formulation between phosphate buffer pH 6.8 and simulated vaginal fluid pH4.2, the similarity factor ($f_2$) was calculated and it was found to be 81.45. Since the $f_2$ values were higher than 50, these results confirmed that the drug release profiles were almost similar for MI3 formulation for both buccal pH and vaginal pH.

**Table 24: *In vitro* dissolution data of MN formulations MF1-MI4 in phosphate buffer pH 6.8**

| Formulation Code | Drug Release (%) | | | | | | | |
|---|---|---|---|---|---|---|---|---|
| | 1 hour | 2 hour | 3 hour | 4 hour | 5 hour | 6 hour | 7 hour | 8 hour |
| | Mean ± S.D* | | | | | | | |
| MF1 | 59.23 ±0.35 | 70.34 ±0.55 | 83.65 ±0.57 | 96.15 ±0.33 | --- | --- | --- | --- |
| MF2 | 80.52 ±0.16 | 91.16 ±0.26 | 99.26 ±0.33 | --- | --- | ---- | --- | ---- |
| MG1 | 30.11 ±0.87 | 53.26 ±1.21 | 75.65 ±0.47 | 90.47 ±0.73 | 94.63 ±0.92 | 98.28 ±0.12 | --- | --- |
| MG2 | 37.36 ±0.89 | 59.27 ±1.01 | 82.34 ±0.96 | 94.54 ±1.25 | 98.11 ±0.21 | --- | --- | --- |
| MH1 | 15.52 ±0.26 | 25.61 ±0.35 | 36.17 ±0.93 | 47.42 ±1.38 | 60.37 ±0.17 | 73.46 ±0.24 | 86.63 ±1.73 | 98.11 ±0.36 |
| MH2 | 13.28 ±0.78 | 23.43 ±0.93 | 29.16 ±0.51 | 38.63 ±0.16 | 54.21 ±1.74 | 70.67 ±0.64 | 78.15 ±0.46 | 90.25 ±0.63 |
| MH3 | 10.25 ±0.64 | 19.23 ±1.46 | 27.38 ±0.45 | 32.22 ±0.35 | 49.25 ±0.26 | 63.24 ±0.45 | 72.52 ±1.45 | 88.28 ±2.16 |
| MH4 | 8.21 ±0.25 | 14.27 ±0.46 | 20.31 ±0.86 | 28.52 ±0.95 | 46.35 ±0.12 | 58.34 ±0.12 | 67.35 ±0.53 | 79.52 ±0.26 |
| MI1 | 42.32 ±0.46 | 45.21 ±0.26 | 54.14 ±0.47 | 65.25 ±0.86 | 83.76 ±0.94 | 94.35 ±0.52 | 96.22 ±0.16 | 98.21 ±0.13 |
| MI2 | 19.15 ±0.36 | 26.27 ±0.12 | 40.41 ±1.26 | 58.27 ±0.52 | 71.11 ±0.27 | 90.21’ ±0.25 | 94.42 ±0.67 | 97.21 ±0.92 |
| MI3 | 18.19 ±0.37 | 25.23 ±0.43 | 38.15 ±0.63 | 56.23 ±0.73 | 67.28 ±0.23 | 81.71 ‘±0.72 | 92.55 ±0.85 | 96.21 ±0.92 |
| MI4 | 15.23 ±0.21 | 20.11 ±0.65 | 34.17 ±0.27 | 50.37 ±0.63 | 61.63 ±0.81 | 75.29 ±0.73 | 90.28 ±0.93 | 94.37 ±0.27 |

***Standard deviation, n = 3**

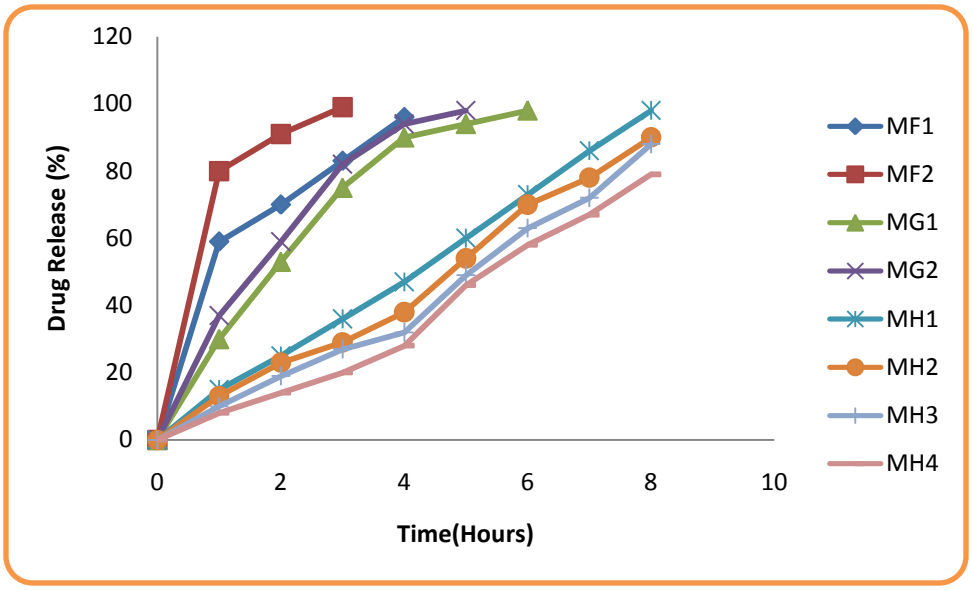


**Figure 60A: MN release profile of formulations MF1-MH4 in phosphate buffer pH 6.8**

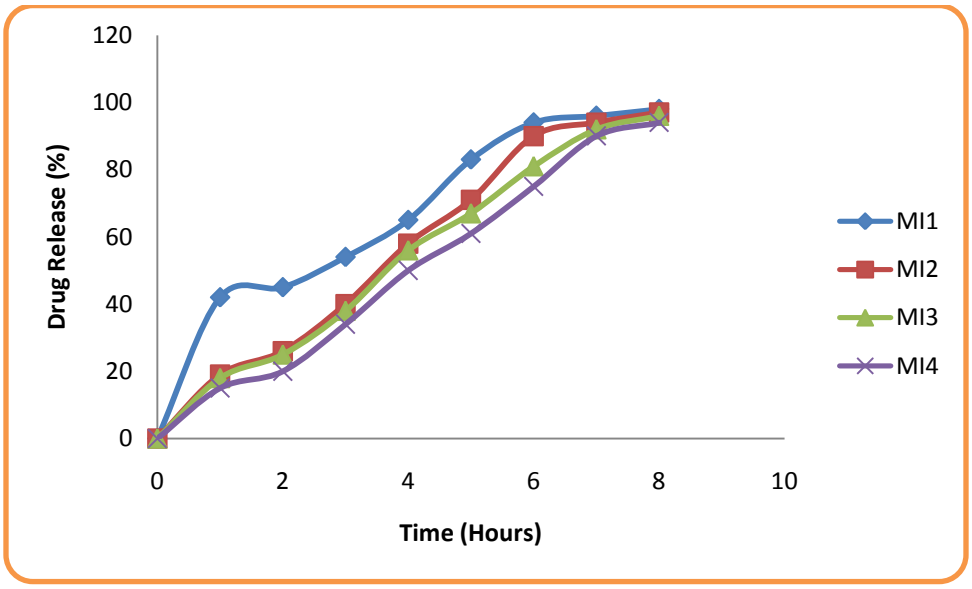


**Figure 60B: MN release profile of formulations MI1-MI4 in phosphate buffer pH 6.8**

**Table 25: *In vitro* dissolution data of MN formulations MF1-MI4 in SVF pH 4.2**

| Formulation Code | Drug Release (%) | | | | | | | |
|---|---|---|---|---|---|---|---|---|
| | 1 hour | 2 hour | 3 hour | 4 hour | 5 hour | 6 hour | 7 hour | 8 hour |
| | Mean ± S.D* | | | | | | | |
| MF1 | 51.12 ±0.43 | 68.52 ±0.57 | 85.63 ±0.13 | 96.17 ±0.37 | -- | --- | --- | --- |
| MF2 | 42.25 ±0.52 | 62.26 ±0.25 | 74.26 ±0.57 | 85.73 ±0.56 | 97.36 ±0.82 | --- | ---- | ---- |
| MG1 | 36.74 ±0.63 | 45.35 ±0.38 | 69.82 ±0.63 | 84.26 ±0.83 | 93.27 ±0.92 | 97.35 ±0.73 | --- | ---- |
| MG2 | 24.37 ±0.77 | 41.27 ±0.72 | 58.86 ±0.37 | 71.25 ±0.27 | 83.11 ±0.24 | 92.67 ±0.29 | 95.25 ±0.24 | --- |
| MH1 | 14.21 ±0.15 | 24.76 ±0.28 | 30.89 ±0.35 | 46.96 ±0.63 | 62.29 ±0.71 | 73.11 ±0.64 | 87.62 ±0.63 | 95.24 ±0.27 |
| MH2 | 12.11 ±0.75 | 21.75 ±0.82 | 27.15 ±0.82 | 36.25 ±0.27 | 54.12 ±0.18 | 69.48 ±0.45 | 79.72 ±0.58 | 92.21 ±0.37 |
| MH3 | 10.13 ±0.28 | 19.36 ±0.29 | 27.96 ±0.57 | 33.26 ±0.73 | 54.17 ±0.82 | 64.36 ±0.39 | 74.21 ±0.94 | 85.19 ±0.35 |
| MH4 | 9.16 ±0.25 | 14.86 ±0.38 | 20.52 ±0.29 | 31.35 ±0.83 | 49.28 ±0.37 | 61.28 ±0.53 | 68.16 ±0.58 | 76.97 ±0.57 |
| MI1 | 23.86 ±0.46 | 30.24 ±0.65 | 42.85 ±0.62 | 54.45 ±0.35 | 62.33 ±0.25 | 75.29 ±0.25 | 81.16 ±0.39 | 85.97 ±0.28 |
| MI2 | 11.26 ±0.35 | 19.75 ±0.36 | 23.25 ±0.29 | 38.73 ±0.38 | 54.93 ±0.34 | 70.38 ±0.14 | 85.36 ±0.84 | 93.92 ±0.38 |
| MI3 | 18.34 ±0.57 | 28.47 ±0.82 | 40.94 ±0.38 | 53.27 ±0.73 | 64.34 ±0.73 | 80.93 ±0.42 | 91.37 ±0.38 | 97.63 ±0.94 |
| MI4 | 15.23 ±0.27 | 24.96 ±0.73 | 37.43 ±0.67 | 50.74 ±0.36 | 62.35 ±0.66 | 76.85 ±0.35 | 90.54 ±0.56 | 95.27 ±0.49 |

***Standard deviation, n = 3**

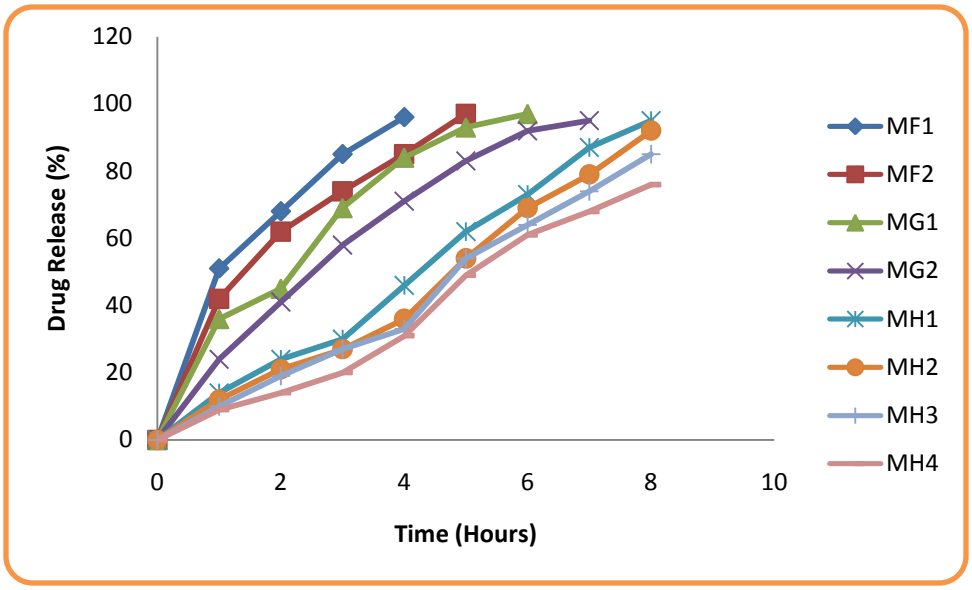


**Figure 61A: MN release profile of formulations MF1-MH4 in SVF pH 4.2**

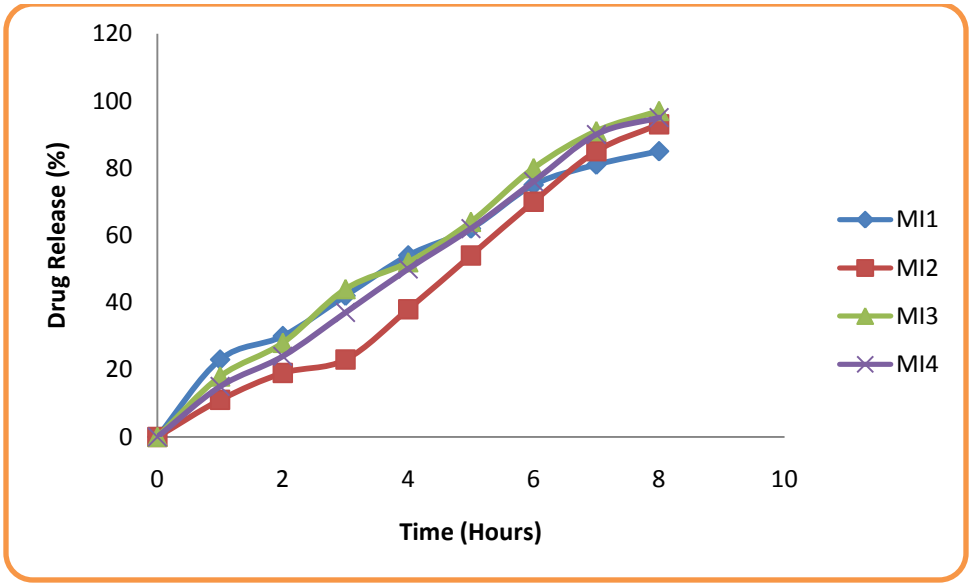


**Figure 61B: MN release profile of formulations MI1-MI4 in SVF pH 4.2**

### 6.2.7 *In vitro* mucoadhesion studies

Mucoadhesive strength for formulations MH1-MI4 are summarized in table 26 and represented in figure 62 respectively. Based on the *in vitro* desired drug release profile, formulations MH1 to MI4 were subjected for mucoadhesive studies. Four formulation containing IPEC exhibited the least mucoadhesive strength. The formed complex lacks the free functional groups which are involved in the complex formation; hence the satisfactory mucoadhesive strength was not evolved. Further increase in the concentration of IPEC, did not increase mucoadhesive strength. The prepared complex lacks the strong binding but slight binding to the mucosal surfaces was observed which may be because of hydrogen bonding interactions [189].

MI1 formulation containing CMT exhibits higher mucoadhesive strength than IPEC formulation; this may be due to the presence of free carboxylic groups. MI2 formulation containing chitosan along with CMT further increased the mucoadhesive strength. MI3 containing higher concentration of CMT exhibited the higher mucoadhesive force than all other formulations. The higher concentration of CMT contains higher carboxylic group that forms tight bond with mucous proteins hence higher mucoadhesive strength.

.

**Table 26: Mucoadhesive strength data for MH1-MI4 formulations**

| Formulation code | Mucoadhesive strength($N/cm^2$) Mean±SD* |
|---|---|
| MH1 | 0.020±0.006 |
| MH2 | 0.03±0.007 |
| MH3 | 0.031±0.007 |
| MH4 | 0.031±0.008 |
| MI1 | 0.07±0.01 |
| MI2 | 0.08±0.01 |
| MI3 | 0.10±0.01 |
| MI4 | 0.08±0.01 |

*mean±SD, n=3

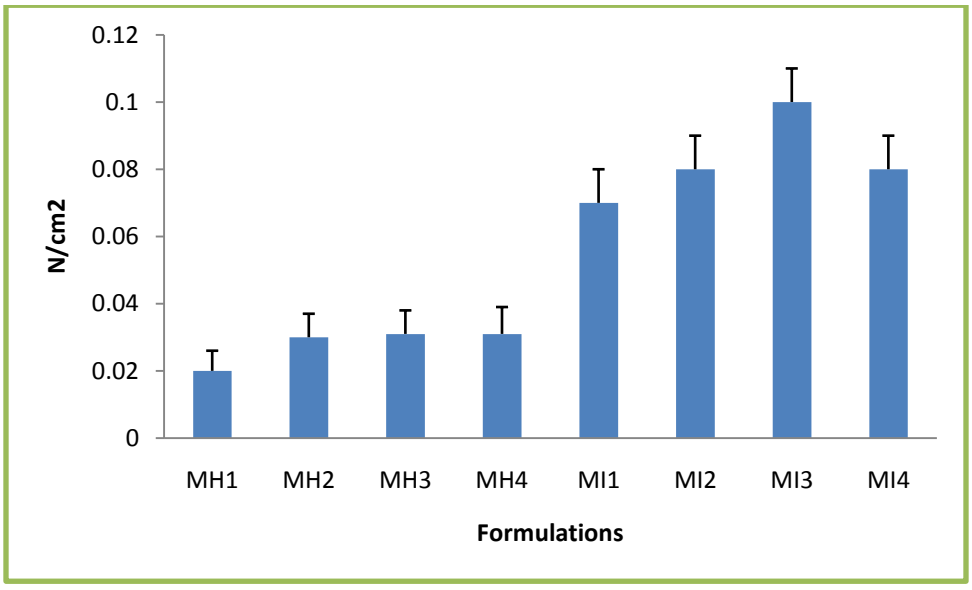


**Figure 62: Mucoadhesive strength profile of formulations MH1-MI4**

### *6.2.8 In vivo* X-ray studies

The bioadhesion & retention property was studied in albino rabbit and X-ray photographic images are given in figure 63. Optimized formulation MI3, developed by using barium sulfate (replacing 50 mg of miconazole) was administered to the rabbit. The duration of tablet in buccal and vaginal cavity was monitored by radiograms. It is evident from the pictures that the tablets showed swelling, remained intact and adhered to the buccal and vaginal mucous membrane for over 8 Hrs.

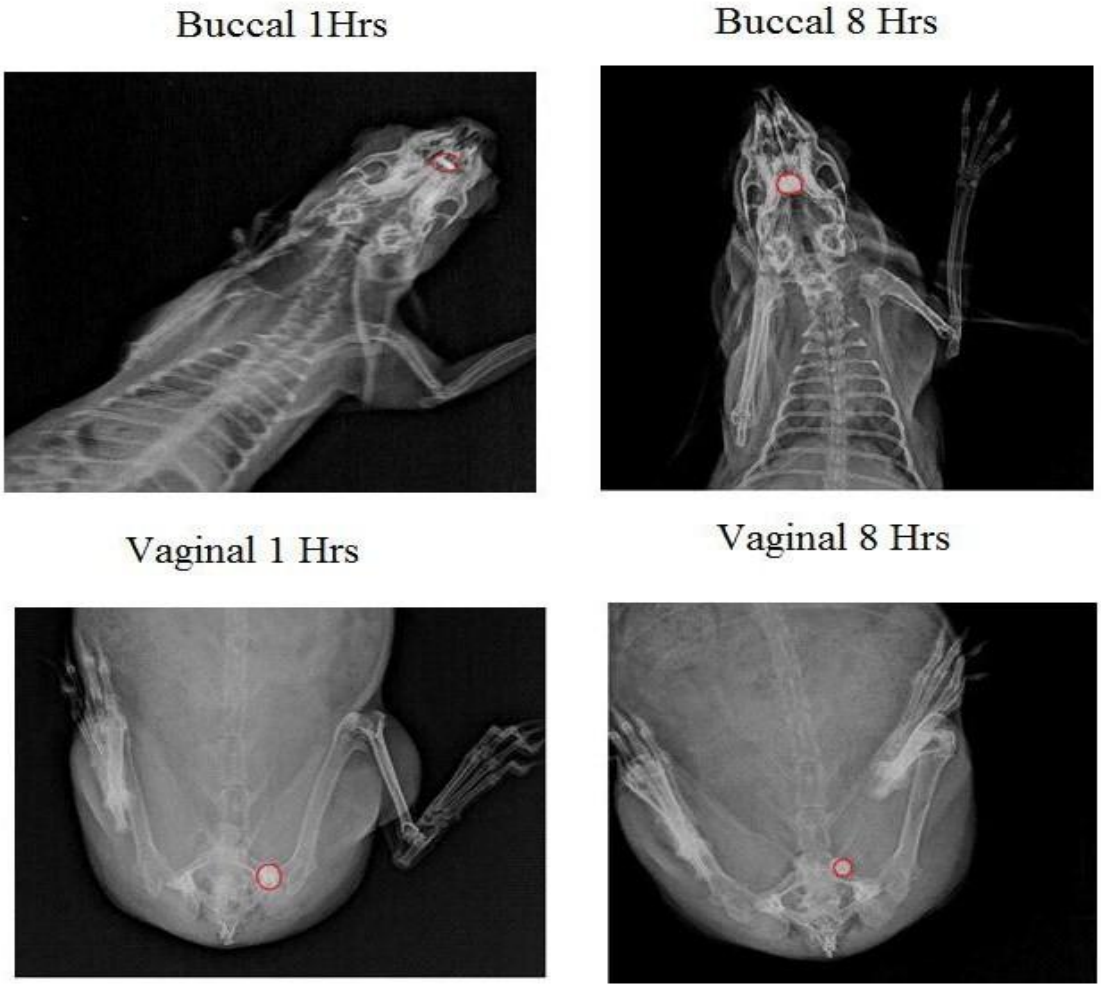


**Figure 63. X-ray radiographic images of buccal and vaginal cavity at 1 and 8 h after ingestion of $BaSO_4$-loaded optimized MI3 matrix tablet in rabbits**

### 6.2.9 Mathematical model fitting

To ascertain drug release mechanism and release rate, the release data were fitted into release models using PCP Disso V2.01 dissolution software. The parameters like 'n' the time exponent and 'R' the regression co-efficient were determined to know the release mechanisms. The data for the formulations MH1-MI4 are summarized in table 27.

**Table 27: Mathematical model fitting data for formulations MH1-MH4**

| Formulation code | Buffer condition | Zero order R | First order R | Matrix R | Peppas | | Hixon crowel R |
|---|---|---|---|---|---|---|---|
| | | | | | R | n | |
| MH1 | Buccal pH | 0.9978 | 0.9422 | 0.9171 | 0.9971 | 0.9973 | 0.9695 |
| | Vaginal pH | 0.9921 | 0.9487 | 0.9182 | 0.9913 | 0.9915 | 0.9427 |
| MH2 | Buccal pH | 0.9929 | 0.9544 | 0.9055 | 0.9920 | 1.0194 | 0.9720 |
| | Vaginal pH | 0.9931 | 0.9815 | 0.9097 | 0.9847 | 0.9408 | 0.9864 |
| MH3 | Buccal pH | 0.9878 | 0.9474 | 0.8870 | 0.9939 | 0.9277 | 0.9644 |
| | Vaginal pH | 0.9910 | 0.9788 | 0.9077 | 0.9847 | 0.9337 | 0.9838 |
| MH4 | Buccal pH | 0.9780 | 0.9433 | 0.8634 | 0.9904 | 0.9255 | 0.9571 |
| | Vaginal pH | 0.9903 | 0.9830 | 0.9028 | 0.9789 | 1.0046 | 0.9860 |
| MI1 | Buccal pH | 0.9397 | 0.9856 | 0.9825 | 0.9634 | 0.5450 | 0.9870 |
| | Vaginal pH | 0.9791 | 0.9893 | 0.9810 | 0.9903 | 0.6537 | 0.9842 |
| MI2 | Buccal pH | 0.9517 | 0.9900 | 0.9855 | 0.9852 | 0.6052 | 0.9924 |
| | Vaginal pH | 0.9926 | 0.9969 | 0.9578 | 0.9954 | 0.8010 | 0.9973 |
| MI3 | Buccal pH | 0.9969 | 0.9686 | 0.9310 | 0.9907 | 0.9551 | 0.9843 |
| | Vaginal pH | 0.9946 | 0.9893 | 0.9201 | 0.9835 | 0.9401 | 0.9918 |
| MI4 | Buccal pH | 0.9951 | 0.9546 | 0.9106 | 0.9878 | 1.0484 | 0.9742 |
| | Vaginal pH | 0.9974 | 0.9950 | 0.9421 | 0.9946 | 0.8799 | 0.9972 |

The MI3 formulation is considered as the best formulation based on the *in vitro* drug release studies and the bioadhesion studies. The best model fit for MI3 formulation is zero order and the n value in peppas model is between 0.9-1 indicating non-fickian diffusion as the release mechanism

### 6.2.10 Stability studies

Stability studies of MN tablet formulation MI3 was carried out to determine the physical stability of the formulation. The stability studies were carried out at 25±2 °C and 60±5 % RH, 30±2 °C and 65±5 % RH and 40±2 °C and 75±5 % RH for 6 months. The MN content in the formulation was evaluated. The observation of conditions is as shown in table 28. There was no significant change in the tablet properties and drug content.

**Table 28: Stability studies data of MI3 formulation**

| **Sampling interval (Months)** | **Stability study conditions** | | |
|---|---|---|---|
| | **25±2 °C & 60±5 % RH** | **30±2 °C & 65±5 % RH** | **40±2 °C & 75±5 % RH** |
| | **% Drug content mean ± S.D*** | | |
| **0** | 99.8± 0.84 | 99.8 ± 0.46 | 99.8 ± 0.74 |
| **3** | 98.1± 0.18 | 98.3 ± 0.27 | 98.5± 0.17 |
| **6** | 97.4± 0.72 | 97.3 ± 0.17 | 97.4 ± 0.25 |

***Standard deviation, n = 3**